

Seeing Through the Dust: Martian Crustal Heterogeneity and Links to the SNC Meteorites

John F. Mustard* and Jessica M. Sunshine†

Through the application of new analytical techniques to high spatial resolution imaging spectrometer data, the ferrous mineralogy of major volcanic terrains on Mars is shown to consist of significant fractions of both low- and high-calcium pyroxene. Changes in the relative abundances of these pyroxenes are observed for units of different age and morphology, even in regions with higher degrees of alteration and contamination from dust. Volcanic rocks with these characteristics are uncommon on Earth but are typical of the basaltic SNC meteorites (shergottites, nakhlites, and chassignites) thought to be from Mars. Thus, it is possible to infer, even through the veil of dust, that the SNC meteorites have mineralogic affinities to major volcanic provinces on Mars and are therefore truly representative of the heterogeneity observed on the surface of the "red planet."

Knowledge of the composition of planetary crusts is fundamental for deducing important stages and processes of planetary evolution. For Mars, our current understanding stems from information gathered from several sources. A mafic to ultramafic composition for Mars is inferred from experiments on the Viking landers that measured the geochemistry of the altered soils and dust (1). There is also abundant morphologic evidence for a complex volcanic history with many contrasting styles (2). Geophysical analyses and modeling provide loose constraints on the bulk composition and thermal evolution of the planet (3). Finally, the SNC meteorites, widely regarded as samples from Mars, provide evidence for early core formation and a long volcanic history (4). Despite the general perspective afforded by these studies, they remain somewhat disconnected. The SNCs, in particular, provide the most detailed data on magmatic processes and crustal composition, yet because actual source areas on the planet for these samples are unknown, we cannot assess how representative of Mars they truly are.

Remote sensing provides a synoptic perspective that can help merge these observations. However, investigations of Mars based on the use of visible to near-infrared reflectance spectroscopy have shown the surface to be dominated by heavily altered, oxidized crust, enriched in poorly crystalline iron oxides (5). Indications of less altered crust have been found (6, 7), but detailed mineralogic assessments are hampered by the low spatial resolution of telescopic data (hundreds of kilometers). In

addition, the pervasive presence of dust at these spatial scales obscures the spectral signatures of the crustal components. These analyses have unfortunately led to the widely held presumption that spectra of the surface of Mars are so dominated by heavily altered dust that fundamental understanding of the composition of the martian crust will only be advanced by data obtained by landers or a sample return mission.

In this report, we present new results made possible by recent advances on two parallel fronts that directly challenge current assumptions about Mars spectroscopy and provide an important geologic context for the SNC meteorites. First, the imaging spectrometer ISM that was on the Phobos II mission in 1989 acquired high spatial resolution (22 km per pixel) and moderate spectral resolution ($\Delta\lambda/\lambda \approx 3\%$) data for $\sim 10\%$ of the planet (8). For the first time, high quality spectral data, from which mineralogic determinations can be made, are available at sufficient spatial resolution that distinct morphogeologic units are resolved. Second, analytic techniques have been developed that allow the relative modal abundances of key mafic minerals to be determined from reflectance spectra (9). Through the application of this new technique to the ISM data, we have been able to directly determine the mafic mineralogy of weakly altered volcanic rocks on Mars. These results indicate the SNC meteorites are in fact representative of major volcanic provinces on Mars.

The spectral data obtained by ISM consist of nine image windows that are ~ 300 km wide and 2000 km long with a spatial resolution of 22 km per pixel. The Tharsis plateau and Valles Marineris regions were well sampled with additional coverage in the Arabia and the Syrtis Major-Isidis regions. A 64-channel reflectance spectrum from 0.77 to 3.14 μm , with a signal-to-noise ratio of $>300:1$, was obtained for each pixel. After data reduction and calibration,

the absolute radiometric accuracy was 10%, and the relative accuracy was better than 0.5% (10). In this analysis, we focus on the wavelength region from 0.77 to 2.55 μm , which includes diagnostic Fe^{2+} crystal field absorptions of the mafic minerals pyroxene and olivine located near 1 and 2 μm (11). Mineralogic assessments are based on the position, strength, and shape of absorption bands in the spectra.

Although much of the martian surface contains a partially obscuring layer of heavily altered material, substantial areas of well-exposed, weakly altered surfaces are recognizable in the ISM data. Contamination of fresh surfaces by alteration typically causes a brightening of materials, a weakening of the strength of ferrous absorption bands, a shift in the 1- μm band center to shorter wavelengths, and a steepened negative continuum. Surfaces that are weakly altered, or relatively "fresh," are thus identified on the basis of these specific combinations of the spectral properties: low albedo, a flat to slightly negative continuum slope, a large 1- μm band area, and a band minimum at wavelengths longer than ~ 0.9 μm . The entire ISM data set has been transformed into a suite of spectral parameters that characterize these properties (12).

Regions identified from the parameter maps that meet the freshness criteria sample geologic units of different age and surface morphology. All show a strong, well-defined absorption near 1.0 μm and an absorption of variable strength and definition near 2.1 μm . The shape, position, symmetry, and strength of the absorptions provide unambiguous identification of calcic pyroxene as a mineral phase on the martian surface (12). However, the spectra also show diversity in the spectral properties of these two dominant absorptions. In general, there are two fundamentally distinct terrains: plateau plains typified by spectra from Nili Patera on Syrtis Major and canyon materials typified by spectra from Eos Chasma in Valles Marineris (Fig. 1).

Compositional analysis of the ISM spectra based on empirically derived correlations between spectral features and chemistry (13) provide unsatisfactory and ambiguous results because the differences in spectral features are consistent with either particle size variations, changes in bulk pyroxene chemistry, variable mixing with altered dust and soil, or variations in the modal abundance of pyroxene and other minerals. To resolve this ambiguity, we used the Modified Gaussian Model (MGM) to deconvolve the ISM reflectance spectra into constituent absorptions (9). The MGM, developed specifically for electronic-transition absorptions, models spectra as a series of absorption bands superimposed on a base line or continuum. The model has

J. F. Mustard, Department of Geological Sciences, Box 1846, Brown University, Providence, RI 02912, USA.
J. M. Sunshine, SETS Technology, 300 Kahalu Avenue, Millitani, HI 96789, USA.

*To whom correspondence should be addressed.

†Visiting scientist, Department of Earth, Atmospheric, and Planetary Sciences, Massachusetts Institute of Technology, Cambridge, MA 02139, USA.

been used successfully to deconvolve overlapping absorptions in mafic mineral mixtures, solid-solution series, and natural lithologic samples (14–16) and is apparently not affected by variations in particle size (14). The parameters defining the absorption bands (center, strength, and width) are quantitatively associated with mineral abundance in mixture series and composition in solid-solution series. Although the weak strengths of mafic mineral absorptions in the ISM data (5 to 15%) make derivation of unique solutions with the MGM difficult, limits on the surface compositions can be determined after critical analysis of results in the context of existing data bases and modeling experience.

Our approach to this problem was to first establish a continuum that is consistent for all model runs. A negative continuum that is linear in energy provides the best approximation to the negative continuum observed for martian dark regions. Using this continuum, we begin with models that make the fewest assumptions about constituents and proceed to more complex models as necessary. The initial absorption band centers for the four models are shown in Table 1. In all trials, the modified stochastic inversion was used (17) and model parameters were minimally constrained (14). The model results are evaluated in terms of their consistency with laboratory investigations (13–15). The following key criteria must be met: (i) the error as a function of wavelength is not systematic, (ii) the band centers of the 1- and 2- μm bands are consistent with laboratory spectra of pyroxenes, (iii) the widths of absorptions are consistent with previous studies, and (iv) when absorption band parameters for two pyroxenes are used (low and high calcium), the relative strengths in the 2- μm region must be comparable to those in the 1- μm region. The results, summarized in Table 2, thus critically depend on simultaneous solutions to the absorptions in both the 1- and 2- μm regions.

It is clear from solutions using either one (model 1 or model 2) or two (model 3 or model 4) pyroxenes that a band near 0.85 μm is required. Models that do not include this band have systematic errors as a function of wavelength between 0.77 and 1.0 μm , typical of a missing absorption, or calculated pyroxene band centers, widths, or strengths that are atypical of known pyroxenes. The band near 0.85 μm is due to ferric-bearing compounds (for example, hematite and ferrihydrite) on the surface. Only one of the four models satisfies all the criteria used to evaluate the solutions (model 4). This model includes high-calcium pyroxene (HCP), low-calcium pyroxene (LCP), and a ferric component. This is the minimum number of mafic minerals that

account for the observed absorptions in the ISM data.

Modeling results for the spectra from Eos and Nili (Fig. 2) provide evidence for clear mineralogic differences in the surface compositions of these terrains. First, the stronger 0.85- μm absorption, as well as a steeper negative continuum, in the spectra of Nili Patera implies a greater ferric component than in Eos. Second, although both spectra include strong LCP and HCP absorptions, the relative strengths of these absorptions differ. Laboratory studies have shown that relative absorption strengths are correlated to the relative modal abundances of these minerals and that this relation is independent of particle size (14). This relation holds in both the 1- and 2- μm regions, and

thus the veracity of the results can be cross-checked by simultaneous analysis of the 1- and 2- μm regions. It is evident from Fig. 2 that the LCP:HCP relative absorption strengths of the 2- μm bands change from ~ 1.28 in Eos to ~ 0.57 in Nili Patera, which corresponds to a $\sim 20\%$ change in the relative model abundance (14).

These differences are comparable to the 11 to 17% change in relative modal abundance detected from analyses of spectra from the two distinct basaltic lithologies (lithologies A and B) in the SNC meteorite EETA 79001 (15). These spectral results are fully consistent with a petrography that shows that lithology A contains approximately 65% pyroxene with an LCP:HCP ratio of 10:1, whereas lithology B contains

Table 1. Initial band centers for MGM models; pyx, pyroxene. The values used for each model were then allowed to vary to best fit the ISM reflectance spectra.

Band center (μm)	Model 1 (one pyx)	Model 2 (one pyx + Fe^{3+})	Model 3 (two pyx)	Model 4 (two pyx + Fe^{3+})
0.85		X		X
0.91	X	X	X	X
1.02			X	X
1.15	X	X	X	X
1.93	X	X	X	X
2.29			X	X

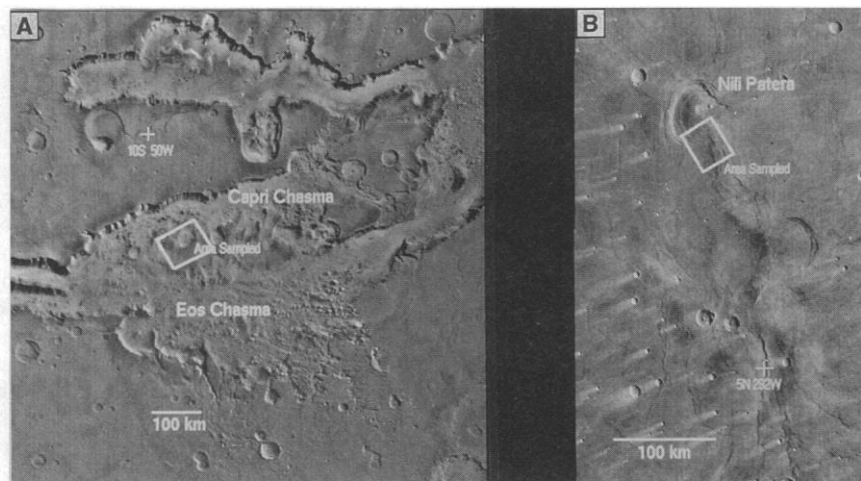
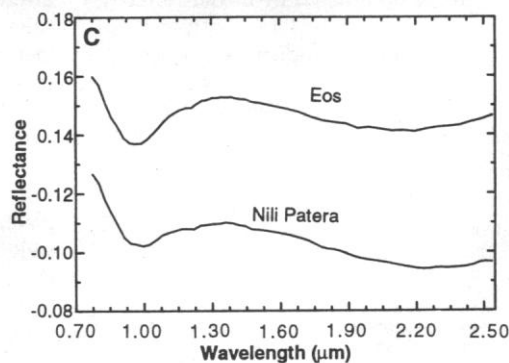


Fig. 1. Location and general geomorphology for the two regions analyzed in detail. Images are from the 1/256° per pixel Mars digital image model produced from Viking Orbiter images by the U.S. Geological Survey. (A) Eos Chasma, which lies within the eastern end of Valles Marineris. The floor of the canyon is ~ 5 km below the surrounding terrain. (B) Nili Patera, a caldera near the center of the Syrtis Major volcanic plateau. The white boxes in (A) and (B) outline the areas for which ISM spectra were extracted for detailed analysis. (C) Reflectance spectra for Eos and Nili.



60% pyroxene with an LCP:HCP ratio of 2:1 (18). Thus, on the basis of our analyses, we conclude that Eos and Nili Patera are two-pyroxene basalts, that LCP is a common, if not dominant, pyroxene phase, and that the primary difference in spectral properties between these terrains is due to a 20% increase in HCP in Nili relative to Eos.

These results were obtained from small regions on Mars exhibiting the least apparent alteration. However, much of Mars exhibits properties intermediate between weakly altered and heavily altered. To determine if the mafic mineralogies inferred for Nili and Eos are common, we selected spectra that are from adjacent regions of the same morphology but that exhibit progressively larger degrees of ferric contamination. The minimum model was applied to each of these spectra, and the results were examined for consistency with the earlier analyses. The mean values of the LCP:HCP ratio of absorption in the 2- μm region [Eos, 1.17 ($n = 5$); Nili, 0.31 ($n = 6$)] provide an estimate of the difference in the abundance of LCP relative to HCP, which corresponds to an enrichment of HCP in the Nili Patera region of approximately 25% relative to Eos Chasma. The standard deviations (Eos, 0.11; Nili, 0.19) represent the spread in values over the regions measured. Although this 25% change in LCP:HCP is slightly greater than the 20% change inferred from the least altered samples, these results clearly show that the mineralogic differences between Syrtis Major (Nili) and Valles Marineris (Eos) are maintained even in the presence of significant degrees of alteration. Using the MGM, we were able to successfully model and remove the effects of variable contamination by weathered materials, allowing the composition of the crust to be evaluated even in the presence of large amounts of alteration. Thus, we can in fact "see through" the dust on Mars.

The modeling of the high spatial resolution spectra from ISM with the MGM demonstrates that there are clear mineralogic differences between the volcanic plains of

Syrtis Major and the volcanic materials on the floor of Valles Marineris. In general, both terrains contain LCP and HCP, likely augite and pigeonite. There is no evidence for abundant olivine present in either area; minor amounts of olivine (<10%) could be present but would not be detected with the current spectral and spatial resolution. The primary difference between the terrains is the relative abundance of pyroxenes; there is ~20% more HCP in the plateau plains volcanics of Nili Patera than in the crustal components on the floor of Valles Marineris.

The mineralogic distinctions between Nili Patera and Eos Chasma are observed over large geographic regions. Exposures of relatively fresh rock throughout Syrtis Major and in Lunae Planum (adjacent to Valles Marineris) are all enriched in HCP, like the volcanics in Nili Patera. Exposures of fresh rock throughout Valles Marineris (Melas, Capri, Coprates chasmata) are enriched in LCP, like the materials in Eos Chasma. Therefore, the voluminous magmatism that produced the plateau plains crystallized rocks that are ~20% enriched in HCP relative to the spatially confined magmatism on the floor of Valles Marineris. In addition, the volcanic materials on the floor of Valles Marineris occur at elevations ~5 km below the ridged plateau plains in a unique tectonic environment. These differences in occurrence and mineralogy are possibly related to changes in source regions. The volcanics of the plateau plains may come from a more fertile source, whereas those in Valles Marineris may indicate a more depleted source.

On the basis of this analysis, we conclude that two-pyroxene basalts with a high proportion of LCP are common on Mars. This result has several important implications. Volcanics of this general nature are not common on Earth, but the SNC meteorites Shergotty, Zagami, EETA 79001, and ALHA 77005 are all two-pyroxene basalts with high proportions of LCP. Longhi and Pan (19) demonstrated that these SNC meteorites crystallized from magmas with ma-

ior element composition analogous to that of terrestrial basaltic komatiites, rare volcanics from the early stages of Earth's history. Our results for the compositions of basaltic terrains on Mars are comparable to those for the SNC meteorites, in that the mafic mineralogies are dominated by two pyroxenes, LCP is abundant, and there is variability in the relative modal abundances, likely associated with the bulk CaO content. The SNCs are small samples from unknown locations on the parent body. Our analyses indicate that there are major volcanic provinces on Mars with these characteristics and that the mineralogic differences are associated with distinct terrains. Therefore, the volcanic compositions of the SNC meteorites appear to be very common on the surface of Mars. By establishing that the SNC meteorites are representative of Mars, we

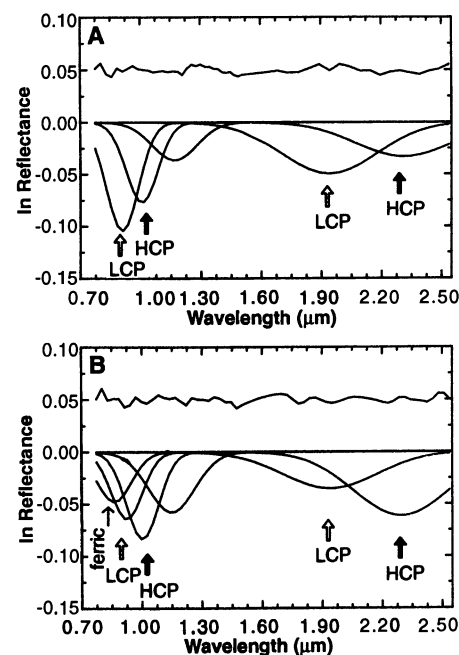


Fig. 2. The fits of MGM model 4 (Table 1) to ISM spectra from (A) Eos Chasma and (B) Nili Patera. In each plot, the residual error between the model spectrum and the data is shown at the top, and the modified Gaussian distributions representing absorptions bands are shown in the lower half. Absorptions associated with LCP are denoted by open arrows, HCP by filled arrows, and the ferric absorption by the narrow arrow (Nili Patera only, no ferric absorption was required for Eos Chasma). The unlabeled absorption near 1.2 μm , although often attributed to plagioclase, is probably associated with both LCP and HCP, as is the case for spectra from the SNC meteorite EETA 79001 (15). Both Nili and Eos have significant fractions of LCP and HCP; yet it is readily apparent that LCP absorptions are stronger than HCP in Eos, whereas the reverse holds true for Nili. This relation is true for both the 1- and 2- μm absorptions. The difference in the relative strengths of LCP and HCP absorptions between Nili and Eos corresponds to a ~20% change in the relative amounts of LCP and HCP.

Table 2. Consistency of model results with known absorption properties of pyroxene and pyroxene mixtures. The symbol Y indicates that the results is consistent, N that it is inconsistent, and n/a that it does not apply. For band centers, the center of the 1- and 2- μm bands must lie within the general filed determined from laboratory spectra (13). The band widths (13, 15) must lie within the general limits identified from analysis of pyroxenes and pyroxene mixtures with the MGM. Error (λ) indicates the wavelength region or regions where a systematic error, indicating an incomplete absorption model, occurs (14, 16). Band strength coupling refers to the fact that the ratio of the HCP to LCP band strengths should be same in the 1- and 2- μm regions if the model is correct (14, 16).

Model	Band centers	Band width		Error (λ) (μm)	Band strength coupling
		1.0 μm	2.0 μm		
1 (one pyx)	N	N	N	2.0, 0.85	n/a
2 (one pyx + Fe ³⁺)	N	Y	N	2.0	n/a
3 (two pyx)	N	Y	Y		N
4 (two pyx + Fe ³⁺)	Y	Y	Y		Y

also solidify the hypothesized compositional link between terrestrial komatiites and martian volcanism (20). The diversity of compositions recognized within the limited spatial coverage of the ISM data set and our demonstrated ability to “see through” the alteration and dust bodes well for expanding our knowledge and understanding of martian crustal compositions and processes from future Mars missions.

REFERENCES AND NOTES

1. B. C. Clark *et al.*, *J. Geophys. Res.* **87**, 10059 (1982).
2. P. J. Mouginis-Mark, L. Wilson, M. T. Zuber, in *Mars*, H. H. Kieffer, B. M. Jakosky, C. W. Snyder, M. S. Matthews, Eds. (Univ. of Arizona Press, Tucson, 1992), chap. 13.
3. G. Schubert, S. C. Solomon, D. L. Turcotte, M. J. Drake, N. H. Sleep, *ibid.*, chap. 5; J. Longhi, E. Knittle, J. R. Holloway, H. Wänke, *ibid.*, chap. 6.
4. H. Y. McSweeney Jr., *Meteoritics* **29**, 757 (1994).
5. T. L. Roush, D. L. Blaney, R. B. Singer, in *Remote Geochemical Analysis: Elemental and Mineralogical Composition*, C. M. Pieters and P. A. J. Englert, Eds. (Cambridge Univ. Press, Cambridge, 1993), pp. 367–394; L. A. Soderblom, in *Mars*, H. H. Kieffer, B. M. Jakosky, C. W. Snyder, M. S. Matthews, Eds. (Univ. of Arizona Press, Tucson, 1992), chap. 17.
6. R. B. Singer and H. Y. McSweeney, in *Resources of Near-Earth Space*, J. Lewis, M. S. Matthews, M. L. Guerrieri, Eds. (Univ. of Arizona Press, Tucson, 1993), pp. 709–736; J. F. Mustard, S. L. Murchie, S. Erard, *Lunar Planet. Sci.* **XXIV**, 1039 (1993).
7. P. Pinet and S. Chevrel, *J. Geophys. Res.* **95**, 14435 (1990).
8. J.-P. Bibring *et al.*, *Nature* **341**, 591 (1989).
9. J. M. Sunshine, C. M. Pieters, S. F. Pratt, *J. Geophys. Res.* **95**, 6955 (1990).
10. S. Erard *et al.*, *Proc. Lunar Planet. Conf.* **21**, 461 (1991).
11. R. G. Burns, *Mineralogic Applications of Crystal Field Theory* (Cambridge Univ. Press, Cambridge, 1993).
12. J. F. Mustard *et al.*, *J. Geophys. Res.* **98**, 3387 (1993).
13. J. B. Adams, *ibid.* **79**, 4829 (1974); E. A. Cloutis and M. J. Gaffey *ibid.* **96**, 18819 (1991).
14. J. M. Sunshine and C. M. Pieters, *ibid.* **98**, 9075 (1993).
15. ———, *Lunar Planet. Sci.* **XXIV**, 1379 (1993); J. F. Mustard, *Am. Mineral.* **1992**, 345 (1992).
16. J. M. Sunshine, L. C. McFadden, C. M. Pieters, *Icarus* **105**, 79 (1993).
17. A. Tarantola and B. Valette, *Rev. Geophys. Space Phys.* **20**, 219 (1982).
18. H. Y. McSweeney and E. M. Stolper, *Geochim. Cosmochim. Acta.* **47**, 1501 (1983).
19. J. Longhi and V. Pan, *Proc. Lunar Planet. Sci. Conf.* **19**, 451 (1991).
20. This link has been proposed by many workers, including T. R. McGetchin and T. R. Smyth [*Icarus* **34**, 512 (1978)], Pinet and Chevrel (7), and D. P. Reyes and P. R. Christensen [*Geophys. Res. Lett.* **21**, 887 (1994)].
21. This manuscript is presented as a tribute to the late Roger G. Burns, whose fundamental research on mineral spectroscopy and martian geochemistry, as well as his encouragement and friendship, played an essential role in our research. We thank P. Hess and M. Rutherford for helpful discussions. This work was supported under National Aeronautics and Space Administration grant NAGW-3379 (J.F.M.).

25 October 1994; accepted 18 January 1995

Direct Observations of Excess Solar Absorption by Clouds

Peter Pilewskie* and Francisco P. J. Valero

Aircraft measurements of solar flux in the cloudy tropical atmosphere reveal that solar absorption by clouds is anomalously large when compared to theoretical estimates. The ratio of cloud forcing at an altitude of 20 kilometers to that at the surface is 1.58 rather than 1.0, as predicted by models. These results were derived from a cloud radiation experiment in which identical instrumentation was deployed on coordinated stacked aircraft. These findings indicate a significant difference between measurements and theory and imply that the interaction between clouds and solar radiation is poorly understood.

Evidence from several experimental and theoretical investigations over the past four decades has shown that the magnitude of shortwave (solar) absorption by clouds is uncertain. There has been some hint that solar absorption is in excess of that predicted by models (1). Cess *et al.* (2) and Ramanathan *et al.* (3) reported that the absorption by the entire atmospheric column in the presence of clouds exceeds model

predictions of absorption by perhaps 35 W m⁻² over the Pacific warm pool (3). The relative error this difference introduces into current theoretical estimates of solar absorption is large, considering that average clear-sky absorption in that region is about 100 W m⁻². The absolute error appears to be small when compared to other terms in the energy budget, but that is misleading. Most of the solar radiation absorbed in the tropics goes toward heating the surface; the remainder, about 20%, helps drive the atmospheric circulation. Thus, what appear to be small errors in absorption by the atmosphere might have huge consequences in tropical atmospheric dynamics. Another consequence of our inability to predict the

magnitude of solar absorption by clouds is the misinterpretation of remote sensing data used to infer cloud microphysical properties. In this report, we present measurements of cloud absorption from the Tropical Ocean Global Atmosphere–Coupled Ocean Atmosphere Response Experiment (TOGA-COARE) and the Central Equatorial Pacific Experiment (CEPEX), based on direct observations from aircraft. For consistency, we present our analysis in a manner similar to that used in (2, 3).

In TOGA-COARE and CEPEX, 20 coordinated flights were made with identical instrumentation above (at an altitude of ~20 km) and beneath (8 to 12 km) cloud layers to determine cloud energetics (that is, flux divergence, absorption, heating, and so on). From TOGA-COARE, 33 hours of useful solar radiation data were acquired during well-coordinated flight segments (aircraft within 0.5°). CEPEX provided an additional 18 hours of well-coordinated solar flux measurements. During both TOGA-COARE and CEPEX, the National Aeronautics and Space Administration (NASA) ER-2 aircraft flew at nearly constant altitude near the tropopause, approximately 20 km; in TOGA-COARE the NASA DC-8 flew at mid-troposphere altitude, between 8 and 12 km, and in CEPEX, the mid-troposphere aircraft was the Aeromet Learjet. Each aircraft was instrumented with two identical broadband (0.3 to 4.0 μm) solar hemispheric field-of-view radiometers (BBHFOV) for simultaneous measurement of upwelling and downwelling flux at both flight levels. Total direct-diffuse radiometers (TDDR) on each aircraft were used to measure spectral components of the solar flux (4, 5).

If one is to determine the absorption in a layer, net solar flux must be acquired simultaneously, or nearly so, at both flight altitudes (Fig. 1). Using the flight navigational data from the DC-8 (or Learjet, for CEPEX) and ER-2 aircraft, we shifted time series of flux data to best align the data sets. Typical time offsets between ER-2 and DC-8 (Learjet) data were less than 3 min, and in most cases the offset was negligible. Therein lies the advance in the TOGA-COARE and CEPEX data sets over the data obtained earlier. Most of the earlier experimental attempts at determining cloud absorption relied on a single aircraft making measurements at several flight altitudes. The reduction to cloud absorption then relied on knowledge of cloud advection, homogeneity, evolution, and so forth. Because flux divergence is obtained from the residual of two relatively large numbers, the net fluxes, coeval measurements are crucial to limiting errors. Some limited attempts have been made at flying stacked aircraft

P. Pilewskie, National Aeronautics and Space Administration Ames Research Center, Moffett Field, CA 94035, USA.

F. P. J. Valero, Atmospheric Research Laboratory, Scripps Institution of Oceanography, University of California at San Diego, La Jolla, CA 92093, USA.

*To whom correspondence should be addressed.